AGU ADVANCING EARTH AND SPACE SCIENCES

Water Resources Research

RESEARCH ARTICLE
10.1029/2024WR039368

A Novel Generalized Semi-Analytical Approach for Flood Control Reservoir Design

Dina Pirone[1], Luigi Cimorelli[1], Andrea D'Aniello[1], and Domenico Pianese[1]

[1]Department of Civil, Architectural and Environmental Engineering, University of Naples Federico II, Naples, Italy

Key Points:

- The proposed approach identifies the maximum outlet discharge that a flood control reservoir can handle for a specific return period
- The approach combines the analytical expression of Flow Duration Reduction with an optimization algorithm to find the critical hydrograph
- The proposed approach shows fast computational times, enabling potential users to explore and compare multiple reservoir configurations

Supporting Information:

Supporting Information may be found in the online version of this article.

Correspondence to:

D. Pirone,
dina.pirone@unina.it

Citation:

Pirone, D., Cimorelli, L., D'Aniello, A., & Pianese, D. (2025). A novel generalized semi-analytical approach for flood control reservoir design. *Water Resources Research*, *61*, e2024WR039368. https://doi.org/10.1029/2024WR039368

Received 18 NOV 2024
Accepted 28 JUL 2025

Author Contributions:

Conceptualization: Dina Pirone, Luigi Cimorelli, Andrea D'Aniello, Domenico Pianese
Data curation: Dina Pirone
Formal analysis: Dina Pirone, Domenico Pianese
Funding acquisition: Domenico Pianese
Investigation: Dina Pirone
Methodology: Dina Pirone, Luigi Cimorelli, Domenico Pianese
Resources: Domenico Pianese
Software: Dina Pirone, Luigi Cimorelli, Domenico Pianese
Supervision: Domenico Pianese
Validation: Dina Pirone, Domenico Pianese
Visualization: Dina Pirone

Abstract Flood control reservoir design requires estimating the total storable water volume or the maximum allowable discharge. This study proposes a novel Generalized Semi-Analytical Approach (GS-AA) to identify the maximum outlet discharge a flood control reservoir can handle for a specific return period. The approach exploits the analytical expression of Flow Duration Reduction (FDR) curves and combines them with an optimization algorithm to find the critical hydrograph and, thus, the hydrograph providing the maximum outlet discharge from the reservoir. The approach models the runoff process of the basin upstream of the reservoir, allowing users to choose any runoff model (RM). The proposed approach shows faster computational times than a fully numerical procedure, enabling potential users to explore and compare multiple reservoir configurations easily. Moreover, this approach addresses flow data limitation issues that prevent FDR curve derivation by correlating them to Intensity Duration Frequency curve parameters, expanding the potential applicability of the procedure in ungauged basins. Finally, results demonstrated the functionality of the procedure regardless of the chosen RM, offering widespread flexibility for users. The proposed GS-AA is a robust and adaptable tool for design and verification purposes to improve flood management strategies.

1. Introduction

Over the past two decades, approximately 4,000 significant flood events have been recorded globally, causing detrimental effects for affected communities (EM-DAT, 2024). These events impacted nearly 1.8 billion individuals, resulting in approximately half a million casualties or injuries and causing an estimated economic loss of around 1 trillion.

Flood control reservoirs have been a topic of significant interest for many years because they offer benefits beyond flood mitigation if a portion of the storable volume is accurately managed (Guo et al., 2024; Schilstra et al., 2024; Zhou et al., 2024). These benefits include water supply during drought periods, recreational activities to stimulate local economies and tourism industries, hydropower generation, renewable energy production, water quality improvement by trapping sediments and pollutants and enhancing downstream water quality (D'Aniello, Cimorelli & Cozzolino, 2019; D'Aniello, Cimorelli, Cozzolino & Pianese, 2019; Kilic, 2024; Tangi et al., 2023; Zhu et al., 2024). Moreover, flood control reservoirs in urban areas face unique challenges due to urbanization, offering resilience against the growing threats of climate change and urban development (Cimorelli et al., 2016; Moazzem et al., 2024). Even though their construction could bring various environmental concerns, such as habitat disruption, alteration of natural water flow, and potential negative impacts on local ecosystems and biodiversity, they are considered an effective measure to reduce peak discharge during flood events (Acreman et al., 2000).

Flood control reservoir design requires estimating the total storable water volume (if the allowable peak discharge downstream of the reservoir is fixed) or the maximum outflow discharge (if the total storable water volume is given). Methods for sizing and verifying flood control reservoirs require a combination of hydrological and hydraulic modeling techniques. Hydrological methods estimate the discharge from the basin upstream of the reservoir (i.e., inflow hydrographs), while hydraulic methods (reservoir routing) simulate how hydrographs propagate through the reservoir of defined characteristics, thus computing the total stored water volume and the maximum outflowing discharge associated with the input hydrographs.

Various hydrological methods can tackle the sizing and verification of flood control reservoirs, each presenting its own set of advantages and drawbacks. These methods include: (a) generating a synthetic series of statistically independent and uniformly distributed flood events as input for the flood control reservoir; (b) considering a

10.1029/2024WR039368

Writing – original draft: Dina Pirone, Luigi Cimorelli, Andrea D'Aniello, Domenico Pianese
Writing – review & editing: Dina Pirone, Luigi Cimorelli, Andrea D'Aniello, Domenico Pianese

design hyetograph; (c) considering a design hydrograph representative of the rainfall-runoff transformations occurring at the upstream basin; (d) considering the Flow Duration Reduction (FDR) curves.

Procedures based on the generation of synthetic flood events provide sufficiently large samples (e.g., hundreds or thousands of years) or ensembles of different time series of the same process to evaluate a wide range of possible outcomes. However, this approach may suffer from uncertainties in model calibration from both rainfall generator and hydrological modeling. Indeed, this approach requires the calibration of numerous parameters for both storm generation models (e.g., Bartlett–Lewis and Neyman-Scott rectangular pulses models or the three-state continuous Markov process occurrence model; Cowpertwait, 1991; Hutchinson, 1990; Rodriguez Iturbe et al., 1987) and rainfall-runoff models (Zoccatelli et al., 2024). Moreover, comprehensive efforts are required to route the generated time series in the reservoir (Cipollini et al., 2022, 2023). For example, Guo et al. (2022) underscored the uncertainty in reservoir flood control systems, emphasizing that understanding and managing uncertainty is crucial for improving the reliability and efficiency of flood control operations. Therefore, these procedures remain applicable and valuable, provided that model parameters are carefully estimated and the inherent uncertainties are clearly quantified and accounted for.

Among the hydrological methods used for flood control reservoir design, the use of design hyetographs and hydrographs offers a practical means to represent typical rainfall or discharge events. These design hyetograph/hydrograph summarize and preserve key physical characteristics and statistical properties of observed time series, enabling simplified yet informative input for evaluating reservoir performance (Gräler et al., 2013). Hyetographs are often preferred over hydrograph estimation because rainfall records are generally quite long and have uniform geographical density, while hydrometric records are often lacking, are not statistically numerous, or include only the annual maximum peak flows (Ganora et al., 2023). Several methods exist to construct a suitable design hyetograph, such as the triangular hyetograph (Yen & Chow, 1980), the Sifalda hyetograph (Sifalda, 1973), the Desbordes hyetograph (Desbordes & Raous, 1980), the Chicago hyetograph (Keifer & Chu, 1957), and the best linear unbiased estimation hyetograph (Veneziano & Villani, 1999). However, the broad range of existing possibilities often creates confusion about the most suitable for a specific study case. Moreover, this approach often overestimates reservoir volumes (Alfieri et al., 2008).

As the NERC (1975) demonstrated that information on the shape of the discharge hydrograph is unnecessary and that incoming volumes are what matter during design, Flow Duration Reduction (FDR) curves (i.e., frequency law of the average volume over the duration with return period T) can be successfully used. In particular, FDR curves provide the maximum value of the average runoff discharge computed over a given duration's time frame. These curves are obtained numerically through the statistical analysis of historical hydrographs or by employing an appropriate inflow-runoff transformation model (for a detailed description of the procedure, interested readers can refer to Tomirotti & Mignosa, 2017). To fully exploit the information of the FDR curves, these can be coupled with a method that searches for the rectangular hydrograph, with uniform intensity during the duration extracted from the FDR, which provides the maximum outlet discharge from the reservoir, defined as the "critical hydrograph" (Pianese & Rossi, 1986a). The advantages of this approach, referred to as "maximizing procedure," lie in the fact that it explores all possible durations and intensities from the FDR curves and is valid regardless of the shape of the hydrograph. Indeed, other studies also corroborate the prevalence of using the rectangular hydrograph shape (Elhassnaoui et al., 2019).

However, direct flow measurements may be affected by various sources of uncertainty, such as rating curve extrapolation, measurement conditions, and equipment limitations (Tomkins, 2014). Moreover, in many cases, the quantity or quality of available data is insufficient for the reliable estimation of FDR curves (Evangelista et al., 2023). Moreover, another drawback of this procedure is that flood routing is numerically solved for all the possible durations of the FDR curves, which is particularly time-consuming. Therefore, searching for the critical inflow hydrograph is not straightforward and challenging. Finally, variational/maximizing approaches may not be physically consistent without suitable relationships between reservoir volumes and discharges at their outlets. These relationships are crucial because they describe how the reservoir behaves under different water levels and flow conditions. Without them, the models might not accurately represent the physical processes governing reservoir behavior, leading to significant errors in discharge predictions. For example, if the model does not account for how changes in water volume affect the rate of discharge at the outlet (due to factors like reservoir geometry or outlet design), it may incorrectly estimate the reservoir's capacity to control floods. This could result in overestimating or underestimating the flood risk, thereby compromising the reliability of flood management

10.1029/2024WR039368

strategies, thus potentially leading to significant errors (Augean South Ltd, 2021; Landfill Guidance Group, 2018; National Coal Board, 1982).

By introducing a new semi-analytical procedure, this study addresses the limitations of the previous approaches by efficiently determining the maximum outlet discharge a reservoir can handle for flood events of a specific return period. First, the proposed approach models the surface runoff of the basin to obtain the analytical expression of the FDR curves from the Intensity Duration Frequency (IDF) curves. Then, for each duration, an analytical resolution for non-linear reservoir routing is used (Pianese & Rossi, 1986a). By coupling the analytical expression of the FDR curves with the analytical solution for non-linear reservoir routing, an analytical expression is obtained. For each rainfall duration, this analytical expression allows for the evaluation of the maximum water volume stored within the reservoir and the maximum outflowing discharge. The expression obtained is implicit and requires a numerical solution. Then, a numerical optimization technique finds the critical hydrograph that provides the maximum discharge outflow from the reservoir and the maximum volume of water stored in it, making the entire procedure much quicker and more efficient. The default approach considers the linear reservoir method to model surface runoff. However, we demonstrate that the procedure is functional regardless of the chosen runoff model. Indeed, the procedure is tested here over five additional runoff models: the Nash model with 2, 3, and 4 reservoirs and the rational method with two different basin shapes (rectangular and circular sector). It is worth noticing that while our method allows flexibility in the selection of the Instantaneous Unit Hydrograph (IUH), the accuracy of the results depends not only on the IUH choice but also on the careful estimation of its parameters. Notably, parameters such as the basin lag time, IDF curve and runoff coefficients are subject to significant uncertainty, despite being widely used and commonly cited in engineering manuals.

Furthermore, the proposed method could address some limitations observed in similar studies on flood control reservoir design. For example, some studies (Manfreda et al., 2021; Volpi et al., 2018) consider an inflow hydrograph with a constant intensity over a single duration derived from IDF curves and adopt reservoir routing solutions valid only for spillway outlets. In contrast, our method explores the full range of possible durations and supports both spillway and bottom outlets. Other studies (Zhao et al., 2020) rely on long post-construction streamflow records, at least 20 years, which are rarely available in ungauged basins. To contrast, our approach could address this time series length requirement using rainfall records. Indeed, our proposed method attempts to correlate FDR curves to IDF curve parameters, which are generally more available. Finally, other studies (Pirone et al., 2024) provided simplified relationships that fit the numerical results of detailed flood-routing simulations but examined only a limited set of reservoir configurations. To contrast, our proposed approach could reduce the computational burden of the numerical implementation of the reservoir routing procedure, thanks to a numerical optimization method, and allow us to investigate all the desired reservoir configurations. By addressing the common limitations across these studies, our proposed method could represent a more comprehensive and practical approach to flood control reservoir design.

2. Theoretical Background

2.1. Reservoir Routing

The propagation of an inflow hydrograph through a reservoir (reservoir routing) involves the solution of a system of three equations: (a) the mass conservation law, expressed in terms of the continuity equation; (b) the energy conservation equation, expressed in the form of an outlet discharge equation; and (c) a relationship describing the changes of water volumes stored in the reservoir as a function of water depth in it.

$$Q_{\text{in}}(\text{t}) - Q_{\text{out}}(t) = \frac{\text{dW}(t)}{\text{dt}} \tag{1}$$

where $Q_{\text{in}}(t)$ and $Q_{\text{out}}(t)$ are the inflow and outflow discharges, $W(t)$ is the water volume in the reservoir (Figure 1), and t is the time. $Q_{\text{out}}(t)$ is generally expressed with an outlet discharge equation (derived from the energy conservation equation), either in tabular form or analytically, Equation 2:

$$Q_{\text{out}}(t) = c\,[h(t)]^n \tag{2}$$

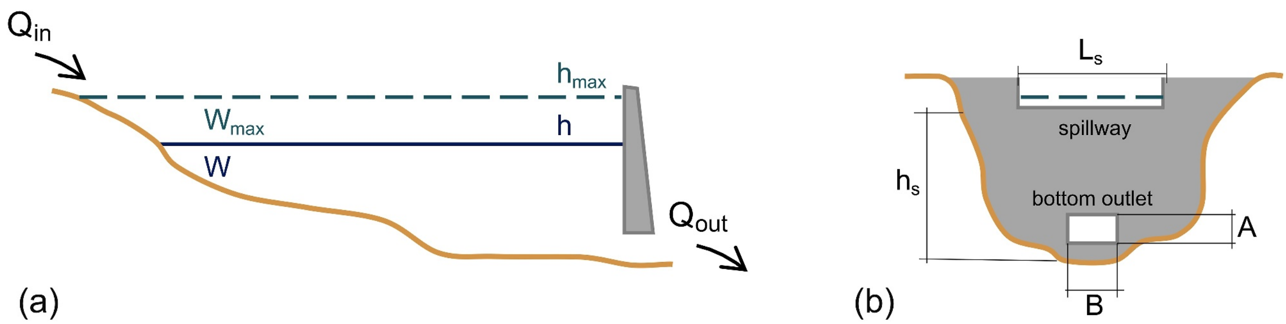

Figure 1. Sketch of a flood control reservoir with a reservoir capacity of W_{max}. (a) Longitudinal section, where Q_{in} is the inflow discharge, Q_{out} is the outflow discharge from the bottom outlet, W is the storage at water level h, and h_{max} is the maximum water level; (b) Cross section, where A and B are the height and the width of the bottom outlet, h_S and L_S are the crest and length of the spillway.

with $h(t)$ the water level in the reservoir at time t, c and n constant values that are determined based on the outlet type and geometry. In particular, for spillways $= \mu_S\, L\, \sqrt{2g}$, $n = 1.5$, $h(t)$ is measured from the crest of the spillway (h_S) of length L (Figure 1) and μ_S is the discharge coefficient, which for spillway is approximately 0.48 (Chow, 1959). For bottom outlets, $c = \mu_B\, \sigma\, \sqrt{2g}$, $n = 0.5$, $h(t)$ is measured from the centerline of the outlet for submerged ones, μ_B is the discharge coefficient, which for bottom outlets is approximately 0.60, and σ is the water section, which for a rectangular section becomes BA, with B and A the width and the height (Figure 1). Finally, g is the gravitational constant.

Conversely, $W(t)$ is generally expressed as a stage-storage relationship, either in tabular form or analytically, Equation 13:

$$W(t) = \alpha\, [h(t)]^{\mathrm{m}} \tag{3}$$

with α and m constant values that are determined based on reservoir type and geometry (m ranges between 1 and 4.5, with 1 being representative of a prismatic geometry with vertical walls, and 4.5 of a more complex morphology with mild lateral slopes; Posey & I, 1940; Manfreda et al., 2021).

The governing storage equations (Equations 1–3) are valid when the water surface is horizontal, thus the outflow is unaffected by tailwater. They can be combined and rewritten to give the following non-linear first-order ordinary differential equation:

$$\upsilon\, K_{\mathrm{res}}\, [Q_{\mathrm{out}}(t)]^{\upsilon-1}\, \frac{\mathrm{d}Q_{\mathrm{out}}(\mathrm{t})}{\mathrm{dt}} + Q_{\mathrm{out}}(\mathrm{t}) - Q_{\mathrm{in}}(t) = 0 \tag{4}$$

where $\upsilon = \frac{\mathrm{m}}{\mathrm{n}}$ and $K_{\mathrm{res}} = \frac{\alpha}{\mathrm{c}^{\upsilon}}$.

Once the inflow hydrograph $Q_{in}(t)$ and the parameters of Equations 2 and 3 are defined, Equation 4 can be solved numerically. However, in some cases, it is also possible to obtain either analytical or approximated solutions, depending on the shape of the inflow hydrograph (Abt & Grigg, 1978; Basha, 1994; Burton, 1980; Culp, 1948; Donahue & McCuen, 1981; Guo, 1999; Hong et al., 2006; Marone, 1964; Pirone et al., 2024; Posey & I, 1940).

Once the solution is achieved, the outflow hydrograph $Q_{out}(\mathrm{t})$, the peak outflow discharge Q^*_{out}, and the maximum volume retained by the reservoir W^* during the flood can be determined (Figure 2). Furthermore, it is also convenient to determine the outflow ratio $\eta = \frac{Q^*_{out}}{Q^*_{in}}$ and the detention ratio $w = \frac{W^*}{W_{in}}$, where Q^*_{in} is the peak inflow discharge, and W_{in} represents the whole flood volume.

2.2. Fully Numerical Approach Coupled With a Maximizing Procedure

Pianese and Rossi (1986a, 1986b) proposed the maximizing procedure, which can be utilized either for design problems (determine the maximum volume of a flood control reservoir required to achieve a desired level of flood reduction downstream) and for verification problems (estimate the maximum outflow discharge from the

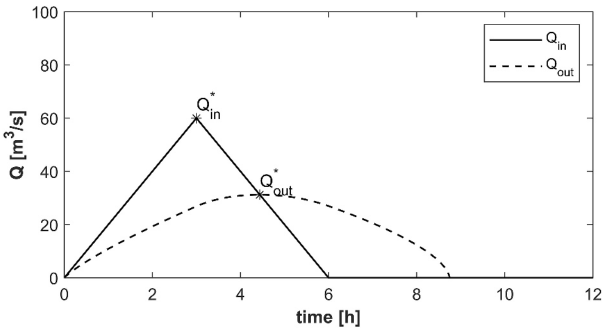

Figure 2. An example of reservoir regulation obtained via numerical resolution of the reservoir routing equations (Equations 1–3). The reservoir parameters used are $c = 5.9798$, $n = 1.5$ (Equation 2), and $\alpha = 3{,}000$, $m = 4$ (Equation 3). Parameter c correspond to a bottom outlet with a square cross-section of 1.5 m × 1.5 m.

reservoir once its design parameters are specified). This procedure assumes that the shape of the flood hydrograph has a negligible role in the sizing/verifying flood control reservoirs if compared to the maximum volumes that can flow into the reservoir in a given time (NERC, 1975).

Therefore, assuming that the flow duration reduction (FDR) curves (Franchini & Galeati, 2000) are known as well as the reservoir parameters (Equations 2 and 3), the maximizing procedure can be summarized as follows:

1. a trial flood duration D is chosen;
2. Q_D is evaluated from the FDR curves;
3. an inlet hydrograph of rectangular shape is considered so that for $t \le D$, $Q_{\text{in}}(t) = Q_D$, and for $t > D$, $Q_{\text{in}}(t) = 0$;
4. Equation 4 is numerically solved; thus, the maximum outflow discharge exiting the reservoir $(Q^*_{\text{out}})_D$, the maximum reservoir volume $(W^*)_D$, and the maximum water level $(h^*)_D$ for the duration D are computed;
5. new flood durations D are set, and the procedure is repeated for each duration from point 2 to point 4.
6. as D varies, the maximum Q^*_{out} among the different values of $(Q^*_{\text{out}})_D$ can be found, together with the respective maximum W^* and h^*, and the corresponding critical flood duration D^* is identified.

It is worth noticing that Pianese and Rossi (1986a, 1986b) verified the reliability of this procedure by comparing the results they obtained through the numerical resolution of Equation 4—regarding some hydrographs of different shapes and durations - with those obtained by first obtaining the FDR curves and then applying the maximizing procedure.

3. Formulation of the Proposed Semi-Analytical Approach

First, Section 3.1 shows how to model the basin's runoff to obtain the analytical expression of the FDR curves. Their estimation requires defining basin parameters such as the IDF curves, the basin area, the impervious area fraction, and the RM. Then, Section 3.2 derives the analytical solution of the reservoir routing equation (Equation 4), which is valid under particular assumptions. Section 3.3 introduces the novel Semi-analytical Approach (S-AA), and the optimization algorithm that quickly provides the maximum outlet discharge from the reservoir. Finally, Section 3.4 generalizes the procedure using other linear and stationary runoff models to derive the Generalized Semi-Analytical Approach (GS-AA).

3.1. Derivation of the Analytical Expression of the FDR Curves for the Linear Reservoir Runoff Model

To obtain the FDR curves analytically from the IDF curves, we transform the input rainfall of different durations into corresponding output runoff hydrographs from the contributing basin. First, we define the IDF curves and the RM. We chose a monotonic expression for the IDF curves:

$$i_{d,T} = a_T\, d^{\beta-1} \tag{5}$$

where a_T is a parameter that depends on the return period, β is a dimensionless parameter, and d is the rainfall duration. Then, we consider rectangular rainfall events with constant intensity I_d during the duration d extracted from the IDF curve.

$$\begin{aligned} I_d(t) &= i_{d,T} = a_T\, d^{\beta-1} && \text{if } t \le d \\ I_d(t) &= 0 && \text{if } t > d \end{aligned} \tag{6}$$

Once the rainfall pattern is known, we use the rational method to evaluate the effective inflow discharge $p(t)$, thus the fraction of precipitation that reaches the basin as surface runoff (Figure 3a):

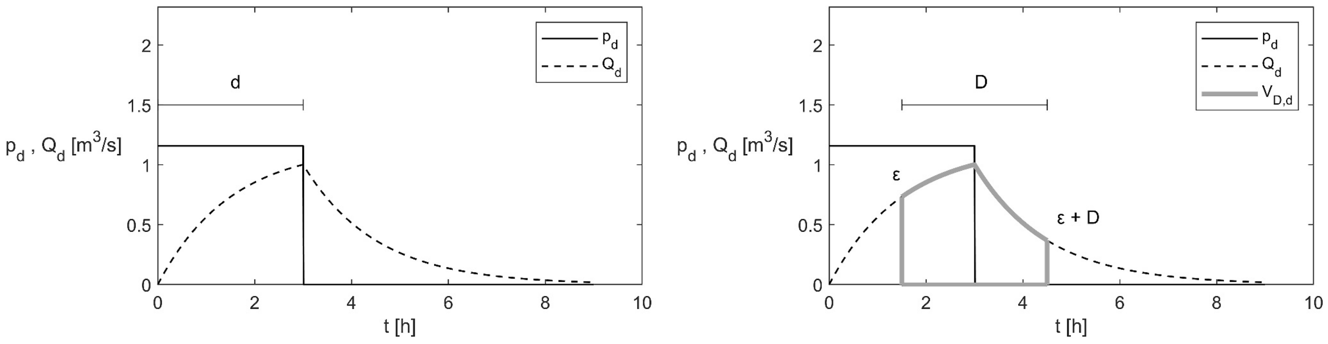

Figure 3. (right) Hydrographs of effective inflow discharge p_d and effective runoff Q_d from the cachment; (left) flood volume $V_{D,d}$ in a time interval of duration D, with ε being the initial instant.

$$\begin{aligned} &p(t) = \varphi\, I_d(t)\, A = \varphi \left(a_T\, d^{\beta-1}\right) A = p_d && \text{if } t \le d \\ &p(t) = 0 && \text{if } t > d \end{aligned} \tag{7}$$

with φ the rational coefficient (representing the fraction of the impervious basin area), and A the basin area.

Assuming the linear reservoir model (LRM) as the RM, the IUH, $u(t)$, and the Unit Hydrograph $S(t)$, can be written as follows:

$$\begin{aligned} u(t) &= \frac{1}{k}\; e^{-\frac{t}{k}} \\ S(t) &= 1 - e^{-\frac{t}{k}} \end{aligned} \tag{8}$$

with k being the basin lag time, which is constant over time.

Since the LRM is linear and stationary, the effective runoff $Q_d(t)$ can be obtained through the convolution integral:

$$Q_d(t) = \int_0^t p(z)\, u(t-z)\, \mathrm{d}z \tag{9}$$

According to Equation 7, the term $p(z)$ is constant and equal to p_d. Thus, Equation 9 becomes:

$$Q_d(t) = p_d \int_0^t u(t-z)\, \mathrm{d}z \tag{10}$$

which can be written as (Figure 3a):

$$\begin{aligned} &Q_d(t) = p_d\, S(t) && \text{if } t \le d \\ &Q_d(t) = p_d\, [S(t) - S(t-d)] && \text{if } t > d \end{aligned} \tag{11}$$

According to Equation 8, Equation 11 becomes:

$$\begin{aligned} &Q_d(t) = R\, d^{\beta-1}\left(1 - e^{-\frac{t}{k}}\right) && \text{if } t \le d \\ &Q_d(t) = R\, d^{\beta-1}\left[\left(1 - e^{-\frac{t}{k}}\right) - \left(1 - e^{-\frac{t-d}{k}}\right)\right] e^{-\frac{t-d}{k}} && \text{if } t > d \end{aligned} \tag{12}$$

where the product $R = a_T \cdot \varphi \cdot A$ is a constant value independent from the rainfall duration and accounting for the return period, the basin imperviousness, and its Area.

10.1029/2024WR039368

The flood volume $V_{D,d}$ that can reach the inlet section of the flood control reservoir in a time interval of duration D can be computed as follows (see Figure 3b):

$$V_{D,d} = \int_{\varepsilon}^{\varepsilon+D} Q_d(t)\,\mathrm{dt} \tag{13}$$

being ε the initial instant.

Solving the integral according to Equation 12, Equation 13 becomes:

$$V_{D,d} = p_d\ k\left[\frac{d}{k} - \frac{\varepsilon}{k} + e^{-\frac{d}{k}} - e^{-\frac{\varepsilon}{k}} + \left(1 - e^{-\frac{d}{k}}\right)\left(1 - e^{-\frac{d}{k}}\, e^{-\frac{\varepsilon+D}{k}}\right)\right] \tag{14}$$

Since the study aims to find the maximum flood volume $V^*_{D,d}$ that can be stored into the reservoir, in a duration D, due to the meteoric event of duration d, the value of ε^* that gives it back needs to be computed. This value is obtained by computing the derivative of Equation 14 for ε and setting it to zero. This operation leads to:

$$\varepsilon^* = k\,\ln\left[1 + e^{-\frac{D}{k}}\left(e^{\frac{d}{k}} - 1\right)\right] \tag{15}$$

By substituting Equation 15 in Equation 14, the maximum flood volume that can arrive at the reservoir inlet over the duration D can be obtained:

$$V^*_{D,d} = p_d\ k\left\{\frac{d}{k} - \ln\left[1 - e^{-\frac{D}{k}}\left(1 - e^{\frac{d}{k}}\right)\right]\right\} \tag{16}$$

Finally, $Q_{D,d}$ can be derived analytically:

$$Q_{D,d} = \frac{V^*_{D,d}}{D} = p_d \frac{k}{D}\left\{\frac{d}{k} - \ln\left[1 - e^{-\frac{D}{k}}\left(1 - e^{\frac{d}{k}}\right)\right]\right\} \tag{17}$$

In turn, the critical rainfall duration d*, which provides the maximum inflow discharge averaged over the duration D, can be determined analytically. This is done by computing the derivative of Equation 17 with respect to the rainfall duration d and setting it equal to zero."

$$\frac{\partial(Q_{D,d})}{\partial \mathrm{d}} = \mathrm{R}\,\frac{\partial}{\partial \mathrm{d}}\left\langle d^{\beta-1}\frac{k}{D}\left\{\frac{d}{k} - \ln\left[1 - e^{-\frac{D}{k}}\left(1 - e^{\frac{d}{k}}\right)\right]\right\}\right\rangle = 0 \tag{18}$$

Developing derivatives and making the necessary simplifications, Equation 18 becomes Equation 19:

$$\frac{e^{\frac{d^*}{k}}}{e^{\frac{D}{k}} - \left(1 - e^{\frac{d^*}{k}}\right)} + (\beta - 1)\,\frac{\left\{\frac{d^*}{k} + \frac{D}{k} - \ln\left[e^{\frac{D}{k}} - \left(1 - e^{\frac{d^*}{k}}\right)\right]\right\}}{\frac{d^*}{k}} - 1 = 0 \tag{19}$$

Once d* is obtained numerically from Equation 19, this value is substituted into Equation 17 to finally obtain the new analytical expression of the FDR curve proposed in this study:

$$Q_D \equiv Q_{D,d^*} = p_{d^*}\frac{k}{D}\left\{\frac{d^*}{k} - \ln\left[1 - e^{-\frac{D}{k}}\left(1 - e^{\frac{d^*}{k}}\right)\right]\right\} \tag{20}$$

The solution is implicit; thus, it should be numerically solved to obtain the analytical expression of the FDR curve (hence the denomination of "semi-analytical approach").

Once the FDR curves are known, they are coupled with the maximizing approach and propagated through the reservoir. In particular, we consider rectangular inflow hydrographs with constant flow Q_D during the duration D extracted from the FDR curve.

3.2. Derivation of the Analytical Solution of the Reservoir Routing Equation

This paper solves the governing storage equations of the reservoir (Equation 4) according to the solution proposed by Pianese and Rossi (1986a). Assuming that, at the initial instant ($t = 0$), the discharge flowing out is equal to the incoming discharge $Q_{out}(t = 0) = Q_{in}(t = 0) = Q_0$ and that the stored volume is known $W(t = 0) = W_0$, thus $W_0 = K_{res} Q_0^{\upsilon}$, Equation 4 can be written as follows:

$$\frac{\upsilon\, W_0}{Q_0^{\upsilon}}\,[Q_{out}(t)]^{\upsilon-1}\,\frac{\mathrm{dQ_{out}}(t)}{\mathrm{dt}} + Q_{out}(t) - Q_{in}(t) = 0 \tag{21}$$

Assuming a rectangular-shaped inflow hydrograph of duration D (so that for $t \le D$, $Q_{in}(t) = Q_D$, and for $t > D$, $Q_{in}(t) = 0$, thus characterized by an incoming volume $W_{in} = D\, Q_D$), Equation 21 is written in dimensionless terms as follows:

$$d\tau = \frac{\upsilon\, w_0}{q_0^{\upsilon}}\,\frac{q_\tau^{\upsilon-1}}{(1 - q_\tau)}\,dq_\tau \tag{22}$$

where $\tau = \frac{t}{D}$, $w_0 = \frac{W_0}{D\, Q_D}$, $q_0 = \frac{Q_0}{Q_D}$, $q_\tau = \frac{Q_{out}(\tau)}{Q_D}$

Developing in geometric series the term $1/(1 - q_\tau)$ and integrating between $\tau = 0$ and $\tau = 1$, Equation 22 becomes:

$$\frac{q_0^{\upsilon}}{w_0} = \sum_{i=0}^{\infty}\left[\frac{\upsilon}{\upsilon + i}\left(q_\tau^{\upsilon+i} - q_0^{\upsilon+i}\right)\right] \tag{23}$$

According to the chosen shape of the inflow hydrograph (rectangular), the peak outflow discharge Q_{out}^{*} and the maximum volume retained by the reservoir W^* during the flood are registered when $\tau = 1$, thus $t = D$ (Figure 3). Moreover, according to the definition of K_{res}, the first term of Equation 23 becomes $\frac{q_0^{\upsilon}}{w_0} = \frac{q_\tau^{\upsilon}}{w_\tau} = \frac{q_\tau^{\upsilon} - q_0^{\upsilon}}{w_\tau - w_0}$. Therefore, to find the outflow ratio η and the detention ratio w, Equation 23 becomes:

$$\frac{1}{w} = \sum_{\mathrm{i}=0}^{\infty}\left\{\frac{\upsilon}{\upsilon + \mathrm{i}}\,\eta^{\mathrm{i}}\,\frac{\left[1 - (\eta_0/\eta)^{\upsilon+\mathrm{i}}\right]}{\left[1 - (\eta_0/\eta)^{\upsilon}\right]}\right\} \tag{24}$$

where $w = w_D - w_0 = \frac{W_D - W_0}{W_{in}} = \frac{K_{res}\, {Q_{out}^{*}}^{\upsilon} - W_0}{D\, Q_D}$ and $\eta_0 = \frac{Q_0}{Q_D}$.

Furthermore, Equation 24 can be rearranged as:

$$D = \frac{W^*}{Q_D}\sum_{\mathrm{i}=0}^{\infty}\left\{\frac{\upsilon}{\upsilon + \mathrm{i}}\,\eta^{\mathrm{i}}\,\frac{\left[1 - (\eta_0/\eta)^{\upsilon+\mathrm{i}}\right]}{\left[1 - (\eta_0/\eta)^{\upsilon}\right]}\right\} \tag{25}$$

and, if $Q_0 = 0$, then Equation 25 becomes:

$$D = \frac{W_D}{Q_D}\sum_{\mathrm{i}=0}^{\infty}\left(\frac{\upsilon}{\upsilon + \mathrm{i}}\,\eta^{\mathrm{i}}\right) \tag{26}$$

It is worth highlighting that Equations 25 and 26 match other studies that evaluated the filling time of a flood control reservoir in the presence of a bottom opening and spillways for stormwater drainage network design (Posey & I, 1940; Supino, 1965, 1967, 1968); Equations 25 and 26 matches also studies that evaluated the filling time of natural rivers when the relationship between the flow cross-sectional area ω and discharge q is expressed as $q = \xi\omega^{1/\upsilon}$, with ξ the discharge coefficient (Cimorelli et al., 2015).

3.3. Maximization Problem Formulation

The maximizing procedure combines the analytical expression of the FDR curve (Equation 20) and the analytical solution of the reservoir routing equations (Equation 26) to find the maximum outflow discharge Q^*_{out} from the reservoir. The maximization problem formulation considers Equation 27:

$$\begin{cases} \text{Max } Q^*_{\text{out}}(D) \\ \text{subjected to} \\ D \geq 0 \end{cases} \tag{27}$$

where the objective function Q^*_{out} is computed as a function of the flood duration D. In detail, the optimization procedure finds the flood duration D that maximizes the outflow discharge from the reservoir as follows. First, it is necessary to define a starting point for the flood duration D, that allows to compute the critical rain duration d^* by solving Equation 19. Once the flood duration D and the critical rainfall duration d^* are known, it is possible to compute the inflow discharge Q_D using Equation 20. Then, according to Equation 26, the attenuation factor η_D with $w_D = K_{\text{res}}[Q^*_{\text{out}}(D)]^{\upsilon}/(D\,Q_D)$ is computed. Thus, the maximum outflow discharge $Q^*_{\text{out}}(D) = \eta_D \cdot Q_D$ is evaluated. Finally, the optimization procedure varies the flood duration D in order to identify the critical one (D^*) that provides the maximum outlet discharge from the reservoir $Q^*_{\text{out}} = \max_D\left[(Q^*_{\text{out}})_D\right]$.

The optimization procedure has been implemented in VB.NET programming language using the Constrained Optimization BY Linear Approximation (COBYLA) algorithm developed by Powell (1994). COBYLA can solve optimization problems with general inequality constraints without resorting to the derivative of the objective function. It performs a sequential linear optimization by linearizing the objective function and the constraints within a specific "trust region" around the current point. The linear approximations of the objective and constraint functions are formed by linear interpolation at $n + 1$ points in the space of the variables and try to maintain a regular-shaped simplex over iterations. In particular, the COBYLA algorithm was implemented within VB.NET using the "csnumerics" library (Gustafsson, 2022)."

3.4. Generalization of the Proposed Semi-Analytical Procedure to Other Runoff Models

The generalization of the proposed semi-analytical procedure to other runoff models is based on two assumptions. The first assumption considers that the shape of the FDR curves of the basin (upstream to the reservoir) is not expected to change significantly as the RM varies (given the same basin characteristics, like Area, lag time, and infiltration model) (Sitterson et al., 2018). The second assumption states that, for linear and stationary runoff models, once the maximum instantaneous inflow discharge Q^*_{in} has been identified, the FDR curves corresponding to each RM could be obtained by appropriately scaling the FDR curve obtained with the LRM.

Therefore, under the assumptions mentioned above, this scaling can be performed by first a-dimensionalizing the FDR curve obtained with the LRM by the maximum instantaneous inflow discharge obtained with it, then multiplying the dimensionless FDR curves by the maximum instantaneous inflow discharge obtained by using any given RM. This scaling procedure is equivalent to multiplying, for each flood duration D, the corresponding discharge Q_D by a correction coefficient CC:

$$\text{CC} = \frac{(Q^*_{\text{in}})_{\text{RM}}}{(Q^*_{\text{in}})_{\text{LRM}}} \tag{28}$$

where $(Q^*_{\text{in}})_{\text{RM}}$ is the instantaneous inflow peak discharge obtained by using any given RM, and $(Q^*_{\text{in}})_{\text{LRM}}$ is the instantaneous inflow peak discharge obtained with the LRM.

Table 1
Parameters List to Compare the Proposed Semi-Analytical Approach and the Fully Numerical Approach

Element	Parameter	Value
IDF curves	a_T [mm/hr]	50
	β	0.25; 0.30; 0.35
Basin	Area [km^2]	100
	Lag time L_t [hr]	3; 4; 5
	φ	0.30
Reservoir	α [m^{3-m}]	3,000; 6,000; 9,000; 18,000
	m	1.0; 1.5; 2.0; 2.5; 3.0; 3.5; 4.0; 4.5
	n	0.5
	c [m^{3-n}/s]	10.63; 16.61; 23.91

Note. The values of c correspond to rectangular shape bottom outlets with cross-section (B × A) = (2.0 m × 2.0 m), (2.5 m × 2.5 m), and (3.0 m × 3.0 m), but also to the cases of $n = 1.5$ and $L = 5.00$ m, $L = 7.81$ m and $L = 11.25$ m, respectively.

4. Verification of the Proposed Procedure: Application Examples

4.1. Comparison Between the Semi-Analytical Approach and the Fully Numerical Approach

To verify the efficacy of the formulated procedure, a comparative analysis was conducted between the proposed S-AA (Section 3.3) and the Fully Numerical Approach (FNA) (Section 2.2) through 864 application examples. These simulations encompass the parameters reported in Table 1, divided into IDF curve parameters (Equation 6), basin parameters (Equation 7), and reservoir parameters (Equations 2 and 3).

The application examples considered three IDF curves corresponding to three common values of exponent β (Equation 6). It is worth noticing that the simulations considered one value for parameter a_T of the IDF curve. This choice is justified because this parameter is independent of the rainfall duration, thus not influencing the derivation of the FDR curves, but it is an amplificative term (as stated in Equation 12). The same justification is valid for parameters Area and φ of the basin. Finally, the simulations considered 96 reservoir configurations by combining the three outlet structure configurations (parameters n and c of Table 1) with the 32 geometry reservoir configurations (parameters α and m of Table 1).

4.2. Generalization of the Proposed Semi-Analytical Procedure to Other Runoff Models

The validity of the generalization of the proposed S-AA was assessed through comparison with five linear and stationary runoff models: the Nash model with 2, 3, and 4 reservoirs (NR 2, NR 3, and NR 4), and the kinematic model with two different basin surface geometries, rectangular shape (named "pitched roof," PR) and circular sector shape (named a "pizza slice," PS). Figure 4 shows the corresponding IUH and Unit Hydrograph S(t) for all the runoff models.

The basin parameters of the additional five runoff models were chosen coherently with the default LRM to ensure a fair and meaningful comparison. Thus, the Area, the basin imperviousness and the Lag Time are the same as in Table 1. In particular, the time of concentration, t_c (Figure 4) of the kinematic model with rectangular shape was set twice the Lag Time, while for the pizza slice shape, it was set 1.5 times the Lag time.

Therefore, starting from the parameters of the IDF curves (Table 1), the FDR curves of each RM were obtained numerically. In particular, the same procedure described in Section 3.1 was used (from Equation 5 to Equation 10), with the difference that the convolutional integral was not solved analytically but numerically, according to the IUH equations in Figure 4.

The comparison between the FDR curves obtained with the six different runoff models is presented in Figure 5. Although peak discharges differ among the FDR curves obtained with the different runoff models, the curves tend to overlap after a duration of approximately three times the lag time.

Moreover, the overlapping of the FDR curves is further confirmed by Figure 6, where the FDR curves are presented in dimensionless form in the plane (δ, r$_\delta$), with $\delta = \frac{D}{L_t}$ and $r_\delta = \frac{Q_D}{Q^*_{in}}$.

4.3. Benchmark Model

The proposed S-AA is tested versus a FNA that does not consider the surface runoff, for which thus the flood duration D equals the rainfall duration d, and thus the Q_D equals p_d. For example, Supino (1965, 1967 and 1968) proposed an analytical expression to evaluate the maximum flow discharge from a flood control reservoir. The expression combines the IDF rainfall curves and a set of decision variables with the flood routing expression to obtain the maximum flow discharge from a reservoir of defined characteristics. Supino's approach allows for fast evaluation of the maximum outflow discharge since the variables can be easily changed (reservoir configuration, outlet geometry, type of material). However, since Supino (1965, 1967 and 1968) neglected the runoff process of the contributing basin area, the results of his approach are realistically oversized.

10.1029/2024WR039368

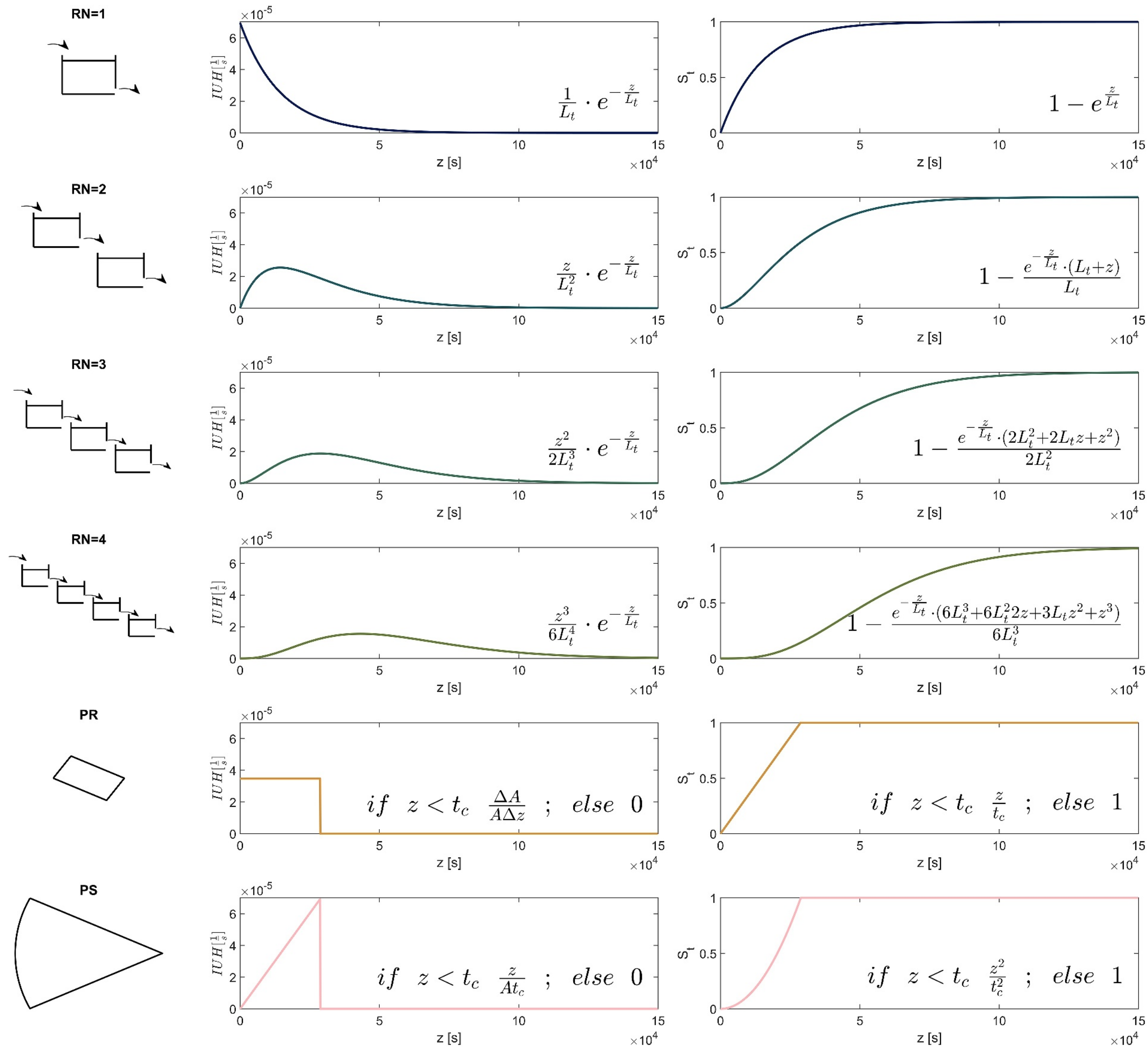

Figure 4. Runoff models used in this study: (left) RM symbols; (central) IUHs and; (right) $S(t)$ and the respective equations.

Therefore, to highlight the importance of modeling the runoff of the basin, we compared the maximum outflow discharge from the reservoir obtained with and without the runoff modeling. In particular, we fixed IDF curves and reservoir parameters; thus we considered one reservoir configuration ($\alpha = 3000, m = 1, n = 0.5, C = 10.63$), one IDF curve configuration ($a_T = 50, \beta = 0.30$), in order to show how the outflow obtained with different methods varied according to basin Areas (from 1 to 200 km^2) and the rational coefficient φ (from 0.2 to 0.5).

5. Results

5.1. Comparison Between the Semi-Analytical Approach and the Fully Numerical Approach

The performance criteria employed to compare the proposed S-AA and the FNA consider the maximum outflow discharge obtained with the two approaches (Equations 29 and 30):

$$\mathrm{Err} = \frac{(Q^*_{\mathrm{out}})_{S-\mathrm{AA}} - (Q^*_{\mathrm{out}})_{\mathrm{FNA}}}{(Q^*_{\mathrm{out}})_{\mathrm{FNA}}} \tag{29}$$

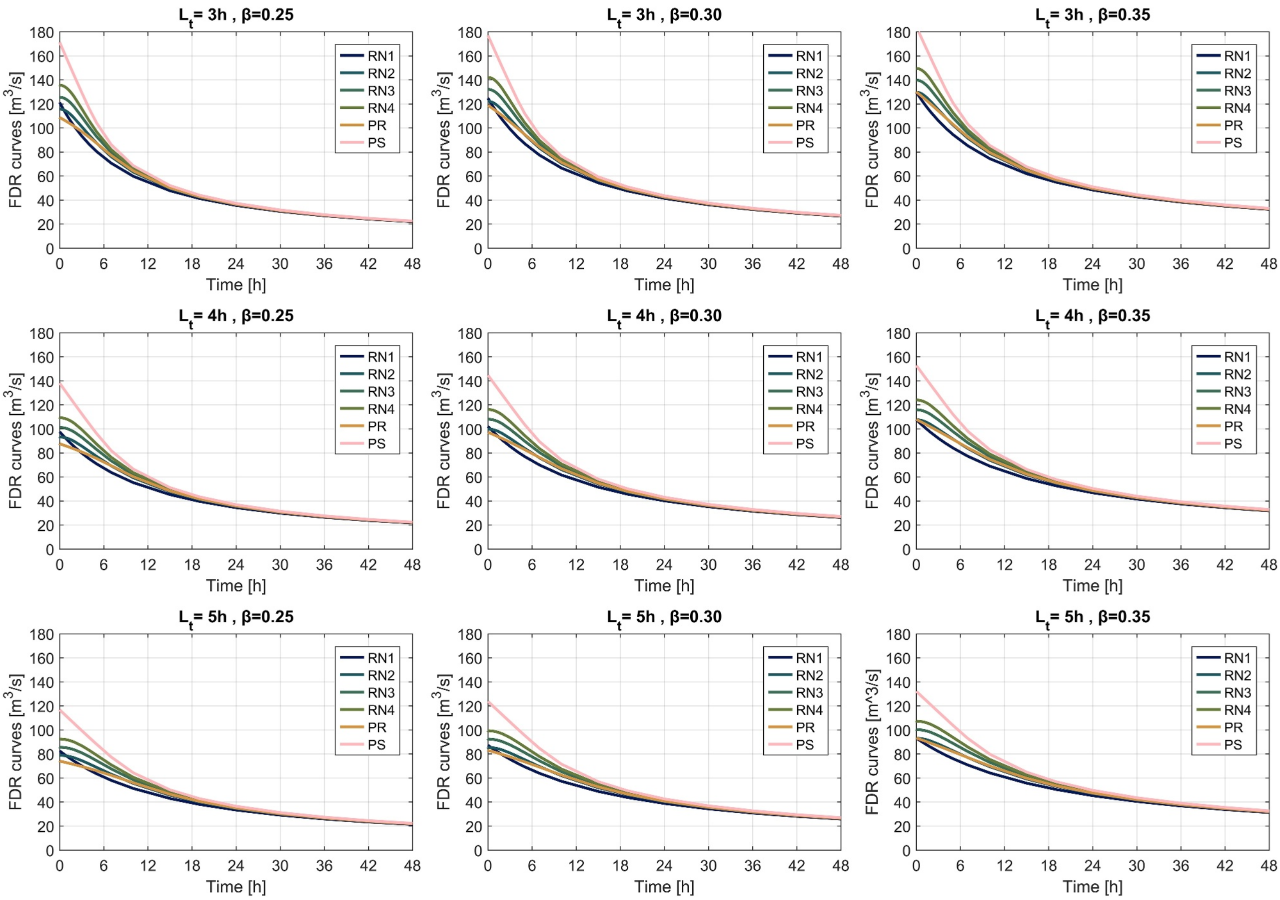

Figure 5. Flow Duration Reduction (FDR) curves obtained according to three Lag Time and three β of the Intensity Duration Frequency curves for six runoff models with parameters of Table 1.

$$\text{RMSE} = \sqrt{\sum_{i=1}^{N} \frac{\{[(Q^*_{\text{out}})_{S-\text{AA}}]_i - [(Q^*_{\text{out}})_{\text{FNA}}]_i\}^2}{N}} \tag{30}$$

where N is the number of application examples.

The errors (Err) between the two approaches are closer to −0.1% and are within the interval −0.5% and 0.05%. In particular, Figure 7 illustrates the histogram of the errors, thus the empirical distribution of errors derived from comparing the two approaches. Notably, within the whole interval −0.5% and 0.05%, most errors (30%) are situated between −0.1% and −0.05%. Furthermore, the empirical distribution exhibits an asymmetrical pattern, with frequencies of errors on the negative axes. Thus, the proposed S-AA tends to slightly underestimate maximum outflow discharges compared to those obtained with the FNA (underestimations less than 0.1% points).

Finally, the RMSE is 1.7524 m^3/s.

5.2. Generalization of the Proposed Semi-Analytical Procedure to Other Runoff Models

The performance indicator employed to compare the GS-AA and the FNA considers the maximum outflow discharge obtained with the two approaches (Equation 31):

$$(\text{Err})_{\text{RM}} = \left[\frac{(Q^*_{\text{out}})_{\text{GS-AA}} - (Q^*_{\text{out}})_{\text{FNA}}}{(Q^*_{\text{out}})_{\text{FNA}}}\right]_{\text{RM}} \tag{31}$$

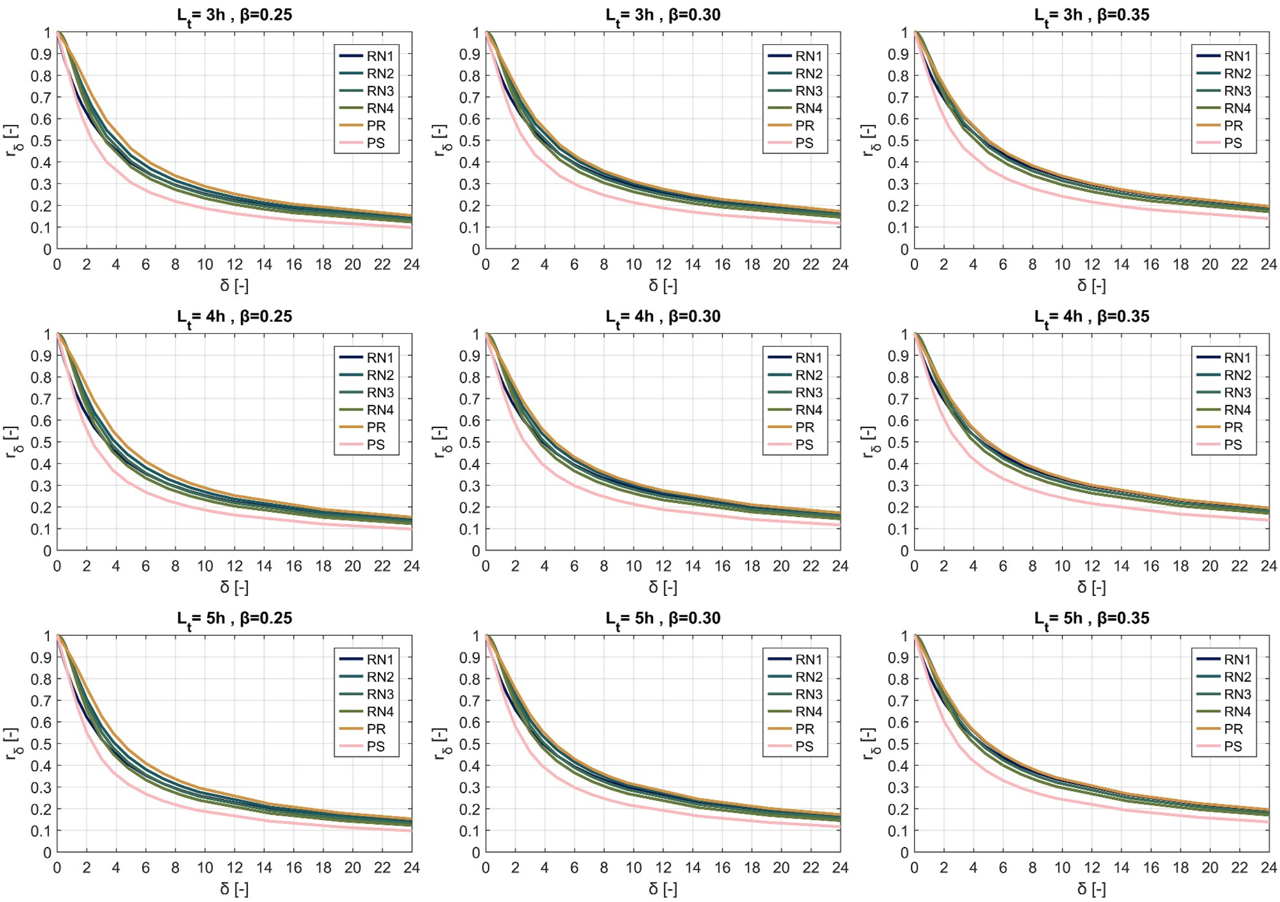

Figure 6. A-dimensionless Flow Duration Reduction (FDR) curves obtained according to three Lag times and three β of the Intensity Duration Frequency curves for six runoff models with parameters of Table 1.

Thus, for each RM, the maximum outflow discharge was computed according to the FNA and compared to those obtained according to the proposed GS-AA (Figure 8). In particular, results are presented by grouping them according to the Lag Time (L_t) and the β value of the IDF curves. Thus, each graph of Figure 8 compares the maximum outflow discharge obtained with the two approaches for 96 reservoir configurations. According to Figure 8, points tend to align along the first quadrant bisector ($x = y$), where each point corresponds to an application example. Notably, most of the points are within the ±10% limits.

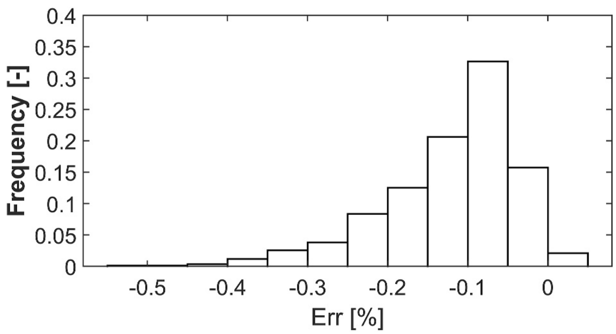

Figure 7. Histograms of the errors (Err) between the proposed Semi-Analytical Approach and the Fully Numerical Approach obtained with Equation 28.

Moreover, Figure 9 shows a graphical representation of the distribution of the errors (Equation 30) for each RM. Once again, results are presented by grouping them according to the Lag Time (L_t) and the β value of the IDF curves. Thus, Figure 9 provides a visual summary of the errors' central tendency, spread, and skewness (Equation 30), as well as the presence of outliers (black points). In particular, errors for the Nash model with 2, 3, and 4 reservoirs (NR 2, NR 3, and NR 4) are within the interval −10% and 0%, highlighting a tendency to underestimate the maximum outflow. Also, the kinematic model with a rectangular shape (named "pitched roof," PR) shows negative errors within the interval −10% and 0%. In contrast, the kinematic model with a circular sector shape (named a "pizza slice," PS) shows errors greater than 0, thus within the interval 0% and 10% intervals.

10.1029/2024WR039368

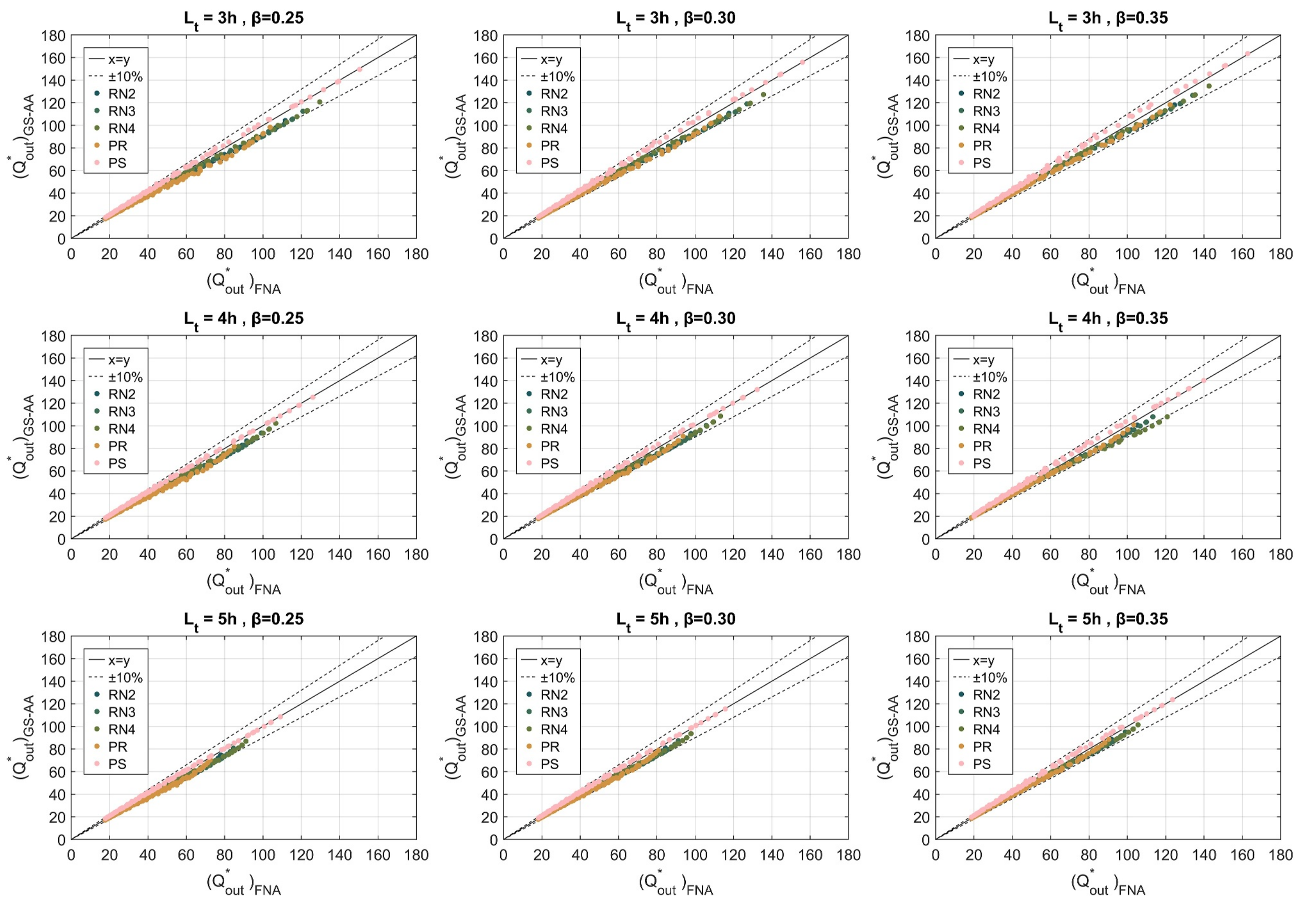

Figure 8. Comparison between the maximum outflow discharge obtained with the Fully Numerical Approach and the proposed Generalized Semi-Analytical Approach. Results are presented by grouping them according to the Lag Time (L_t) and the β value of the Intensity Duration Frequency curves. Colors follow recommendations of scientifically derived color maps (Crameri et al., 2020).

5.3. Benchmark Model

The performance criteria employed to compare the proposed S-AA and the above-described benchmark model that does not model basin runoff (NR, meaning No Runoff) consider the ratio between the maximum outflow obtained by modeling the runoff of the basin with the LRM and the one obtained without modeling the runoff (NR).

$$(Q^*_{\mathrm{out}})_{\mathrm{ratio}} = \frac{(Q^*_{\mathrm{out}})_{\mathrm{NR}}}{(Q^*_{\mathrm{out}})_{\mathrm{LRM}}} \tag{32}$$

Results are shown according to different values of the basin area (from 1 to 200 km^2), four values of the rational coefficient φ ($\varphi = 0.20$; $\varphi = 0.30$; $\varphi = 0.40$; $\varphi = 0.50$) and regarding the same reservoir configuration ($\alpha = 3000, m = 1, n = 0.5, C = 10.63$) (Figure 10).

For basin areas lower than 10 km^2, the outflow computed without modeling the runoff is almost four times the outflow obtained with the proposed approach. As the basin area increases, this ratio tends to align along the value of three. Moreover, regarding the same basin area value, the ratio on the y-axis increases as the rational coefficient decreases.

6. Discussions

This study formulated a novel GS-AA that efficiently provides the maximum outlet discharge of a reservoir of defined characteristics for a given return period. The proposed S-AA formulation allows for addressing the

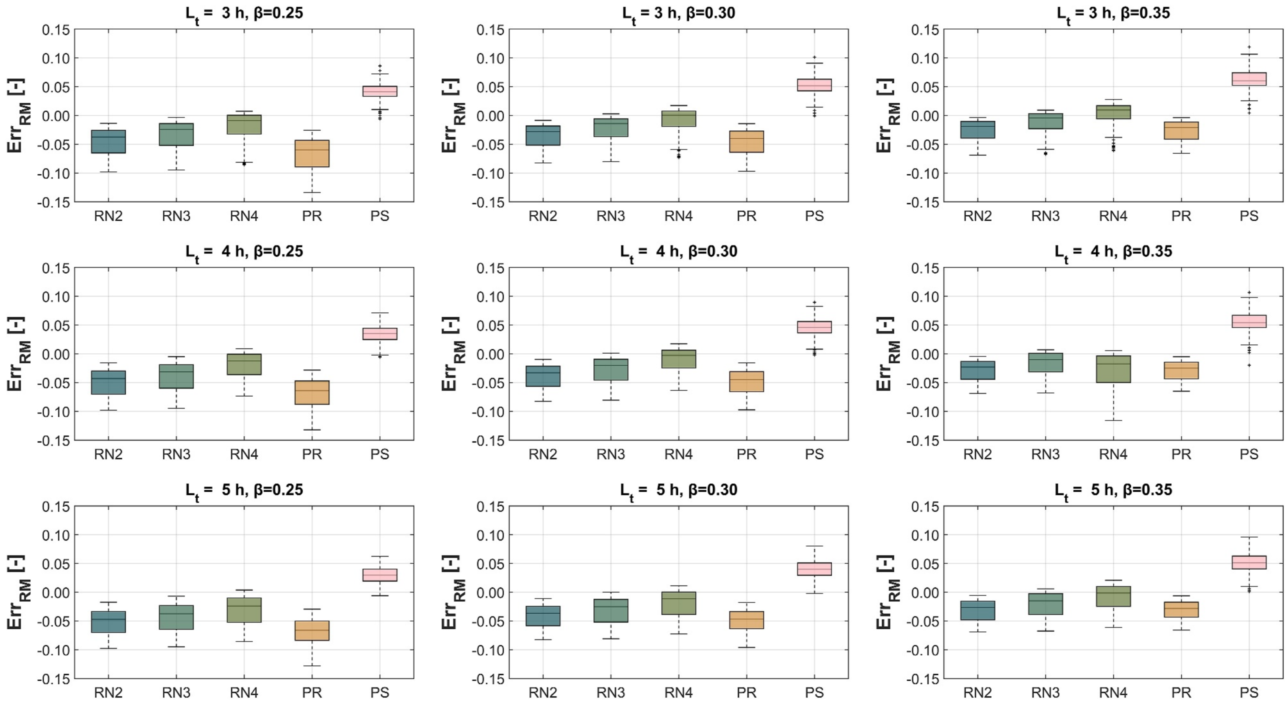

Figure 9. Boxplots showing the errors (Equation 30) between the maximum outflow discharge obtained with the Fully Numerical Approach and the proposed Generalized Semi-Analytical Approach. Results are presented by grouping them according to the Lag Time (L_t) and the β value of the Intensity Duration Frequency curves. In each graph and for each runoff model (x-axis), the boxplot of the errors is shown. In particular, each boxplot shows five summary statistics: minimum, first quartile (Q1), median (second quartile, Q2), third quartile (Q3), and maximum, represented as black horizontal lines.

following issues. First, the approach addresses flow data limitation issues that prevent Flood Duration Reduction (FDR) curve derivation by correlating them to IDF parameters, which are more widespread. This correlation enhances accessibility and expands the potential applicability of the procedure across regions and watersheds where reliable flow data may be scarce. Moreover, it gives the possibility to evaluate the FDR curves concerning different values of return period by simply changing the parameter a of the IDF curve (Equation 5). For example, this broader reach is particularly advantageous in ungauged basins where traditional methods relying on direct flow measurements may not be feasible or in the case when there are strict requests on the flow record length, at least 20 years after the reservoir construction (Zhao et al., 2020). On the other hand, to evaluate the FDR curves, the proposed RM requires just two parameters (lag time and runoff coefficient), which have a clear physical meaning, have been widely studied in the literature, and thus can be easily evaluated in any context. For an example of the GS-AA application to an existing reservoir, given the IDF curve and basin upstream of the reservoir parameters, please refer to the Supporting Information S1.

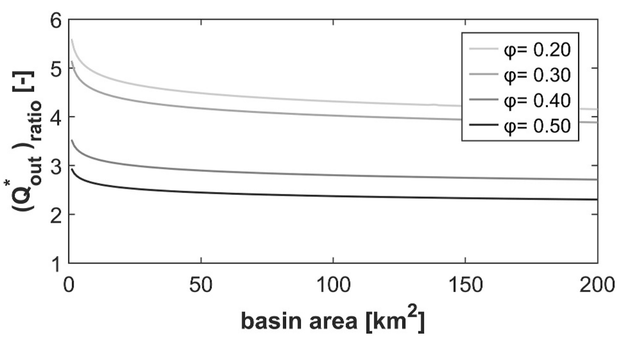

Figure 10. The ratio between the maximum outflows from the reservoir obtained with the proposed Semi-Analytical Approach and without modeling the basin's runoff versus the basin area, according to different rational coefficients (φ) regarding the same reservoir configuration ($\alpha = 3000, m = 1, n = 0.5, C = 10.63$).

The S-AA also reduces computational times associated with the numerical implementation of complete reservoir routing procedures. Indeed, the proposed procedure stands out for its notably short computation times compared to the FNA. In this study, a FNA application required an average processing time of three hours, utilizing a high-performance computing setup featuring an Intel Core i9 11th generation processor with a clock velocity of 3.7 GHz and a Max Turbo Frequency of 5.3 GHz. The system had a robust storage configuration, including a 2,000GB SSD hard disk, specifically the ADATA 3,500/3,000 MB7S 2TB NVME model. In contrast, the proposed SS-A provided instantaneous results, eliminating the need to wait for computational time. This result is a crucial feature of the proposed procedure that allows to efficiently explore and compare several reservoir configurations for design and verification problems with incomparable speed. In contrast, previous studies proposed simplified relationships to identify the reduction effect of a reservoir. However, these relationships are recommended during preliminary evaluation since they approximate numerical simulation, and they are valid under strict assumptions regarding inflow hydrograph, incoming flood volumes and for specific reservoir configuration (Pirone et al., 2024; Sordo-Ward et al., 2013). Moreover, the remarkable reduction offered by our method in computational time could be essential for flood risk assessment procedures, thus allowing for quicker decision-making processes. Finally, it is also reassuring that errors between the S-AA and the FNA are minimal (as depicted in Figure 4), often amounting to mere percentage points.

Results demonstrated the functionality of the procedure regardless of the chosen RM, offering considerable flexibility for potential users. The analysis also showed that the choice of the RM has practically scarce influence on evaluating the maximum outflow discharge from the reservoir. Indeed, results indicated close agreement between the two approaches (Figure 8). This agreement suggests high consistency and accuracy in the discharge computations across different scenarios. Furthermore, most errors fall within the ±10% limits (Figure 9), emphasizing the robustness and reliability of the proposed GS-AA. In this way, a potential user can freely model the surface runoff of the basin upstream of the reservoir to compute the peak discharge and then use the G-SAA - thanks to the correction coefficient (Equation 28)—to estimate the maximum discharge outflow of the reservoir. For example, similar studies that developed different runoff models for the upstream basins (Volpi et al., 2018) could use them and exploit the proposed procedure's rapidness.

Moreover, it can be confirmed that the assumptions underpinning the generalization of the proposed semi-analytical procedure to other runoff models have been validated (Section 3.4). The first assumption, which states that the shape of the FDR curves remains relatively consistent across different runoff models for the same basin characteristics, has been supported (Figures 8 and 9). Additionally, the errors on the peak discharge between the two procedures have confirmed the correctness of the second assumption about the scalability of FDR curves obtained with the LRM for other linear and stationary runoff models (Figures 8 and 9). Thus, these validated assumptions support the reliability and applicability of the proposed GS-AA procedure to provide accurate estimations of maximum outflow discharge with different runoff models.

Finally, results highlighted that neglecting runoff phenomena leads to significant overestimations of flood control reservoir maximum outflow discharge, especially for small basins. Indeed, these overestimations sharply increase as the basin area decreases. In contrast, as the basin area increases, overestimations decrease. These trends confirm that the influence of runoff is more pronounced in smaller basins. In contrast, in larger basin areas, other factors such as storage capacity and flow dynamics could become more dominant in influencing outflow discharge, reducing the relative importance of runoff in the overall system behavior. Therefore, neglecting the runoff process of the upstream basin could hinder effective resource allocation and flood management planning, potentially exacerbating the economic waste.

7. Conclusions

The proposed GS-AA provides valuable insights into flood control reservoir designing, allowing users to explore and compare several reservoir configurations for both design and verification problems. Moreover, the proposed approach establishes a correlation between the FDR and IDF curve parameters, addressing the flow data scarcity issue and enhancing the procedure potential applicability, particularly in ungauged basins. The proposed GS-AA also fully exploits the information of the FDR curves by combining them with an analytical solution of the reservoir routing equations and a maximizing procedure. The procedure uses an optimization algorithm to quickly find the critical hydrograph, with uniform intensity extracted from the FDR curves, which provides the maximum outlet discharge from the reservoir. The optimization algorithm sharply reduces computational times associated with implementing the fully numerical procedure. Moreover, results demonstrated the procedure usefulness regardless of the chosen RM, offering widespread flexibility for users. Accounting for the runoff of the basin and its impact on reservoir sizing and verification can give more information for effective decision-making processes regarding water allocation, ecosystem management, and infrastructure planning. Additionally, as climate change continues to alter precipitation patterns and intensify hydrological processes, incorporating accurate representations of runoff basins becomes increasingly vital for developing resilient water management strategies. Finally, the proposed approach represents a probabilistic and flexible tool to support the design of flood control reservoirs, enabling more efficient exploration of design alternatives and. Contributing to more informed and adaptive flood management strategies.

Appendix A: Notation

Table A1

Table A2

Table A1
Latin Symbols

Symbol	Description
A	Height of the bottom outlet
a_T	Parameter of the IDF curve
B	Width of the bottom outlet
c	Constant value varying according to reservoir outlet type (Equation 2)
$\mathrm{CC} = \frac{(Q_{\mathrm{in}}^{*})_{\mathrm{RM}}}{(Q_{\mathrm{in}}^{*})_{\mathrm{LRM}}}$	Correction coefficient to generalize the proposed approach with a different runoff model
D	Flood event duration
d	Rainfall event duration
d^{*}	Critical rainfall duration
Err	Performance indicator employed to compare the S-AA and the FNA
$\mathrm{Err}_{\mathrm{RM}}$	Performance indicator employed to compare the GS-AA and the FNA
g	Gravitational constant
h	Water level in the reservoir
$(h^{*})_D$	Maximum water level in the reservoir related to an inflowing hydrograph with a rectangular shape characterized by a duration equal to D
I_d	Rainfall intensity of duration d extracted from the IDF
$i_{d,T}$	Rainfall intensity of the IDF curve
k	Basin lag time
$K_{\mathrm{res}} = \frac{\alpha}{c^{\upsilon}}$	Coefficient depending on the water volume stored in the reservoir and discharge outflowing from outlets
L	Overflow length
L_t	Lag time of the basin
m	Constant value varying according to reservoir type and geometry (Equation 3)
n	Number of application example
n	Constant value varying according to reservoir outlet type and geometry (Equation 2)
p	Effective inflow discharge
p_d	Inflow discharge generated from the rainfall event
Q_0	Discharge flowing out the reservoir at time 0
$q_0 = \frac{Q_0}{Q_D}$	Dimensionless discharge flowing out of the reservoir at time 0
Q_D	Flow discharge extracted from the FDR curve with duration D
$Q_{D,d}$	Mean flow discharge obtained over the duration D from a rectangular hyetograph of duration d and intensity extracted from the IDF curve
Q_d	Effective runoff of the basin
Q_{in}	Inflow discharge of the reservoir
Q_{in}^{*}	Peak inflow discharge
$(Q_{\mathrm{in}}^{*})_{\mathrm{LRM}}$	Instantaneous inflow peak discharge obtained with the linear reservoir model (LRM)
$(Q_{\mathrm{in}}^{*})_{\mathrm{RM}}$	Instantaneous inflow peak discharge obtained by using any given runoff model (RM)
Q_{out}	Outflow discharge of the reservoir
Q_{out}^{*}	Peak outflow discharge
$(Q_{\mathrm{out}}^{*})_D$	Maximum discharge outflowing from reservoir related to an inflowing hydrograph with a rectangular shape characterized by a duration equal to D
$(Q_{\mathrm{out}}^{*})_{\mathrm{LRM}}$	Maximum outflow discharge obtained with the Linear Reservoir Model

Table A1
Continued

Symbol	Description
$(Q^{*}_{\mathrm{out}})_{\mathrm{FNA}}$	Maximum outflow discharge obtained with the Fully Numerical Approach
$(\mathrm{Q}^{*}_{\mathrm{out}})_{\mathrm{NR}}$	Maximum outflow discharge obtained without modeling the Runoff of the basin
$(Q^{*}_{\mathrm{out}})_{S-\mathrm{AA}}$	Maximum outflow discharge obtained with the proposed Semi-Analytical Approach
$(Q^{*}_{\mathrm{out}})_{\mathrm{ratio}}$	Ratio between the maximum outflow obtained by modeling the runoff of the basin with the Linear Reservoir Model (LRM) and the one obtained without modeling the runoff (NR)
$q_{\tau} = \frac{\mathrm{Q}_{\mathrm{out}}(\tau)}{\mathrm{Q}_{\mathrm{D}}}$	Dimensionless outflow discharge
$R = a_{T} \cdot \varphi \cdot \mathrm{Area}$	Constant value of Equation 12
$\mathrm{r}_{\delta} = \frac{Q_{\mathrm{D}}}{Q^{*}_{\mathrm{in}}}$	Dimensionless FDR curves
S	Unit hydrograph
T	Return period
t	Time
t_{c}	Time of concentration of the kinematic model
u	Instantaneous Unit Hydrograph
W	Water volume in the reservoir
$w = \frac{W^{*}}{W_{\mathrm{in}}}$	Detention ratio
W_{0}	Volume stored in the reservoir at time 0
$w_{0} = \frac{W_{0}}{D\,Q_{D}}$	Dimensionless volume stored in the reservoir at time 0
$w_{d} = \frac{K_{\mathrm{res}}\left[(Q^{*}_{\mathrm{out}})_{d}\right]^{\upsilon}}{D\,Q_{D}}$	Dimensionless volume stored in the reservoir generated by a rainfall event of duration *d* and intensity extracted from the IDF curve
W_{in}	Incoming flood volume
W^{*}	Maximum water volume in the reservoir
$(W^{*})_{D}$	Maximum volume stored in the reservoir related to an inflowing hydrograph with rectangular shape characterized by a duration equal to *D*
$V_{D,d}$	Flood volume that can reach the inlet section of the flood control reservoir in a time interval of duration *D* related to a rainfall event with rectangular shape and duration *d*
$V^{*}_{D,d}$	Maximum flood volume that can reach the inlet section of the flood control reservoir in a time interval of duration *D* related to a rainfall event with rectangular shape and duration *d*

Table A2
Greek Symbols

Symbol	Description
α	Constant value varying according to reservoir type and geometry (Equation 3)
β	Parameter of the IDF curve
$\delta = \frac{D}{L_{t}}$	Dimensionless time
ε	Initial instant of Equation 13
ε^{*}	Initial instant that provides the maximum flood volume $\mathrm{V}^{*}_{D,d}$
$\eta = \frac{Q^{*}_{\mathrm{out}}}{Q^{*}_{\mathrm{in}}}$	Outflow ratio
$\eta_{0} = \frac{Q_{0}}{Q_{D}}$	Outflow ratio of the initial time 0
$\eta_{\mathrm{D}} = \frac{(Q^{*}_{\mathrm{out}})_{D}}{Q_{D}}$	Outflow ratio related to a flood event of duration *D*
μ	Discharge coefficient
φ	Rational coefficient
$\tau = \frac{t}{D}$	Dimensionless time
$\upsilon = \frac{m}{n}$	Exponent in the relationship between the water volume stored in the reservoir and discharge outflowing from outlets

Data Availability Statement

The code developed to formulate the Generalised Semi-Analytical Approach (GS-AA) is openly available at Zenodo via (Pirone, 2024) https://doi.org/10.5281/zenodo.14180291.

Acknowledgments
This study was carried out within the RETURN Extended Partnership that received funding from the European Union Next-GenerationEU (National Recovery and Resilience Plan—NRRP, Mission 4, Component 2, Investment 1.3—D.D. 1243 2/8/2022, PE0000005). Open access publishing facilitated by Universita degli Studi di Napoli Federico II, as part of the Wiley - CRUI-CARE agreement.

References

Abt, S., & Grigg, N. (1978). Approximate method for sizing detention reservoirs. *Journal of Water Resources*, *14*(4), 956–965.
Acreman, M., Farquharson, F. A. K., McCartney, M. P., Sullivan, C., Campbell, K., Hodgson, N., et al. (2000). Managed flood releases from reservoirs: Issues and guidance. *Report to DFID and the World Commission on Dams. Centre for Ecology and Hydrology*, 86.
Alfieri, L., Laio, F., & Claps, P. (2008). A simulation experiment for optimal design hyetograph selection. *Hydrological Processes: International Journal*, *22*(6), 813–820.
Augean South Ltd. (2021). Surface water management plan for the proposed extended East Northants resource management facility. Report reference au/kcw/jrc/20032/01swmp, July).
Basha, H. (1994). Non-linear reservoir routing: Particular analytical solution. *Journal of Hydrologic Engineering*, *120*(5), 624–632.
Burton, K. R. (1980). Stormwater detention basin sizing. *J. Hydraulic Div., ASCE*, *106*(3), 437–439.
Chow, V. T. (1959). *Open-channel hydraulics*. McGraw-Hill.
Cimorelli, L., Cozzolino, L., D'Aniello, A., Morlando, F., & Pianese, D. (2015). A simplified approach for stormwater drainage networks sizing. *J Climatol Weather Forecasting*, *3*, 136. https://doi.org/10.4172/2332-2594.1000136
Cimorelli, L., Morlando, F., Cozzolino, L., Covelli, C., Della Morte, R., & Pianese, D. (2016). Optimal positioning and sizing of detention tanks within urban drainage networks. *Journal of Irrigation and Drainage Engineering*, *142*(1), 04015028.
Cipollini, S., Fiori, A., & Volpi, E. (2022). A new physically based index to quantify the impact of multiple reservoirs on flood frequency at the catchment scale based on the concept of equivalent reservoir. *Water Resources Research*, *58*(2), e2021WR031470. https://doi.org/10.1029/2021WR031470
Cipollini, S., Volpi, E., & Fiori, A. (2023). Toward a catchment-scale assessment of flood peak attenuation by multiple reservoirs. *Water Resources Research*, *59*(2), e2022WR032821. https://doi.org/10.1029/2022WR032821
Cowpertwait, P. S. P. (1991). Further developments of the Neyman-Scott clustered point process for modelling rainfall. *Water Resources Research*, *27*(7), 1431–1438.
Crameri, F., Shephard, G. E., & Heron, P. J. (2020). The misuse of colour in science communication. *Nature Communications*, *11*(1), 5444.
Culp, M. (1948). The effect of spillway storage on the design of upstream reservoirs. *Journal of Agricultural Engineering*, *29*, 344–346.
D'Aniello, A., Cimorelli, L., & Cozzolino, L. (2019b). The influence of soil stochastic heterogeneity and facility dimensions on stormwater infiltration facilities performance. *Water Resources Management*, *33*, 2399–2415.
D'Aniello, A., Cimorelli, L., Cozzolino, L., & Pianese, D. (2019a). The effect of geological heterogeneity and groundwater table depth on the hydraulic performance of stormwater infiltration facilities. *Water Resources Management*, *33*(3), 1147–1166.
Desbordes, M., & Raous, P. (1980). Fondaments de l'élaboration d'une pluie de projet urbaine. Méthodes d'analyse et applicationa la station Montpellier Bel Air. La Météorologie, VI série (Vol. *20*, pp. 317–326).
Donahue, R. J., & McCuen, R. H. (1981). Comparison of detention basin planning and design models. *J. Water Res. Plann. Manag. Div., ASCE*, *107*(2), 385–400.
Elhassnaoui, I., Moumen, Z., Serrari, I., Bouziane, A., Ouazar, D., & Hasnaoui, M. D. (2019). Generation of synthetic design storm hyetograph and hydrologic modeling under HEC HMS for Ziz watershed. *International Journal of Innovative Technology and Exploring Engineering*, *8*(10), 2278–3075.
EM-DAT. (2024). Retrieved from https://public.emdat.be/data
Evangelista, G., Ganora, D., Mazzoglio, P., Pianigiani, F., & Claps, P. (2023). Flood attenuation potential of Italian dams: Sensitivity on geomorphic and climatological factors. *Water Resources Management*, *37*(15), 6165–6181.
Franchini, M., & Galeati, G. (2000). Comparative analysis of some methods for deriving the expected flood reduction curve in the frequency domain. *Hydrology and Earth System Sciences*, *4*(1), 155–172.
Ganora, D., Evangelista, G., Cordero, S., & Claps, P. (2023). Design flood hydrographs: A regional analysis based on flood reduction functions. *Hydrological Sciences Journal*, *68*(2), 325–340.
Gräler, B., van den Berg, M. J., Vandenberghe, S., Petroselli, A., Grimaldi, S., De Baets, B., & Verhoest, N. E. C. (2013). Multivariate return periods in hydrology: A critical and practical review focusing on synthetic design hydrograph estimation. *Hydrology and Earth System Sciences*, *17*(4), 1281–1296.
Guo, A., Chang, J., Wang, Y., Wu, B., & Li, Y. (2022). Tracing design flood hydrograph uncertainty in reservoir flood control system. *Applied Mathematical Modelling*, *102*, 371–384. https://doi.org/10.1016/j.apm.2021.09.012
Guo, C. Y. (1999). Detention storage volume for small urban catchments. *J. Water Res. Plann. Manag., ASCE*, *125*(6), 380–382.
Guo, Y., Xu, Y. P., Yu, X., Liu, L., & Gu, H. (2024). AI-based ensemble flood forecasts and its implementation in multi-objective robust optimization operation for reservoir flood control. *Water Resources Research*, *60*(5), e2023WR035693. https://doi.org/10.1029/2023WR035693
Gustafsson. (2022). Csnumerics repository. Retrieved from https://Github.Com/Cureos/Csnumerics
Hong, Y.-M., Yeh, N., & Chen, J.-Y. (2006). The simplified methods of evaluating detention storage volume for small catchment. *Ecological Engineering*, *26*, 355–364.
Hutchinson, M. F. (1990). A point rainfall model based on a three-state continuous Markov occurrence process. *Journal of Hydrology*, *114*(1–2), 125–148.
Keifer, C. J., & Chu, H. H. (1957). Synthetic storm pattern for drainage design. *Journal of the Hydraulics Division*, *83*(4), 1332.
Kilic, M. (2024). Estimation of future hydropower generation of reservoir systems used for different purposes in different regions. *IET Renewable Power Generation*.
Landfill Guidance Group. (2018). Sizing of surface water management systems at landfill sites. *Industry Code of Practice no. LGG 116, Vers.*, *1*, 37.
Manfreda, S., Miglino, D., & Albertini, C. (2021). Impact of detention dams on the probability distribution of floods. *Hydrology and Earth System Sciences*, *25*, 4231–4242. https://doi.org/10.5194/hess-25-4231-2021
Marone, V. (1964). Calcolo di massima dell'effetto di laminazione di un serbatoio sulle piene. *L'Energia Elettr*, *46*, 1–8.

Moazzem, S., Bhuiyan, M., Muthukumaran, S., Fagan, J., & Jegatheesan, V. (2024). A critical review of nature-based systems (NbS) to treat stormwater in response to climate change and urbanization. *Current Pollution Reports*, 1–26. https://doi.org/10.1007/s40726-024-00297-8

National Coal Board. (1982). Technical management of water in the coal mining industry. *NCB Mining Department*, 129.

NERC. (1975). Flood studies report (Vol. *1*).

Pianese, D., & Rossi, F. (1986a). Curve di possibilità di laminazione delle piene (Flood attenuation possibility relationships). *Giornale del Genio Civile, Fascicolo 4°-5°-6° - Aprile – Maggio – Giugno*, 131–148. (in italian).

Pianese, D., & Rossi, F. (1986b). Reservoir storage-flood peak attenuation relationships. *EXCERPTA of the Italian Contributions to the Field of Hydraulic Engineering*, *1*, 73–79.

Pirone, D. (2024). A novel generalised semi-analytical approach for flood control reservoir design. *[CODE] Zenodo*. https://doi.org/10.5281/zenodo.14180291

Pirone, D., Cimorelli, L., & Pianese, D. (2024). The effect of flood-mitigation reservoir configuration on peak-discharge reduction during preliminary design. *Journal of Hydrology: Regional Studies*, *52*, 101676. https://doi.org/10.1016/j.ejrh.2024.101676

Posey, C. J., & I, F.-T. (1940). Functional design of flood control reservoirs. *Trans. ASCE*, *105*(1), 1638–1674. paper 2093. https://doi.org/10.1061/TACEAT.0005281

Powell, M. J. (1994). *A direct search optimization method that models the objective and constraint functions by linear interpolation* (pp. 51–67). Springer.

Rodriguez-Iturbe, I., Cox, D. R., & Isham, V. (1987). Some models for rainfall based on stochastic point processes. *Proceedings of the Royal Society of London, Series A: Mathematical and Physical Sciences*, *A*(410), 269–288.

Schilstra, M., Wang, W., van Oel, P. R., Wang, J., & Cheng, H. (2024). The effects of reservoir storage and water use on the upstream–downstream drought propagation. *Journal of Hydrology*, *631*, 130668. https://doi.org/10.1016/j.jhydrol.2024.130668

Sifalda, V. (1973). Entwicklung eines Berechnungsregens für die Bemessung von Kanalnetzen. *GWF - Wasser/Abwasser*, *114*(H9), 435–440.

Sitterson, J., Knightes, C., Parmar, R., Wolfe, K., Avant, B., & Muche, M. (2018). An overview of rainfall-runoff model types.

Sordo-Ward, A., Garrote, L., Bejarano, M. D., & Castillo, L. G. (2013). Extreme flood abatement in large dams with gate-controlled spillways. *Journal of Hydrology*, *498*, 113–123. https://doi.org/10.1016/j.jhydrol.2013.06.010

Supino, G. (1965). *Le Reti Idrauliche* (pp. 227–231). Casa Editrice Pàtron.

Supino, G. (1967). Il metodo del Volume di invaso e la moderazione delle piene nelle reti idrografiche – Osservazioni generali – Calcolo dei serbatoi (The "Accumulating Volume Method" and flood attenuation in drainage networks – General observations – Sizing of flood attenuation reservoirs). *Il Giornale del Genio Civile*, 719–736.

Supino, G. (1968). Limitazione delle piene con due serbatoi in serie – Scarichi a battente e a stramazzo (Flood attenuation by two tanks in series – Bottom openings and weirs). *Il Giornale del Genio Civile*, 3–22.

Tangi, M., Bizzi, S., Schmitt, R., & Castelletti, A. (2023). Balancing sediment connectivity and energy production via optimised reservoir sediment management strategies. *Water Resources Research*, *59*(6), e2022WR034033. https://doi.org/10.1029/2022WR034033

Tomirotti, M., & Mignosa, P. (2017). A methodology to derive synthetic design hydrographs for river flood management. *Journal of Hydrology*, *555*, 736–743. https://doi.org/10.1016/j.jhydrol.2017.10.036

Tomkins, K. M. (2014). Uncertainty in streamflow rating curves: Methods, controls and consequences. *Hydrological Processes*, *28*(3), 464–481.

Veneziano, D., & Villani, P. (1999). Best linear unbiased design hyetograph. *Water Resources Research*, *35*(9), 2725–2738.

Volpi, E., Di Lazzaro, M., Bertola, M., Viglione, A., & Fiori, A. (2018). Reservoir effects on flood peak discharge at the catchment scale. *Water Resources Research*, *54*(11), 9623–9636. https://doi.org/10.1029/2018WR023866

Yen, B. C., & Chow, V. T. (1980). Design hyetographs for small drainage structures. *Journal of the Hydraulics Division*, *106*(6), 1055–1076.

Zhao, G., Bates, P., & Neal, J. (2020). The impact of dams on design floods in the conterminous US. *Water Resources Research*, *56*(3), e2019WR025380. https://doi.org/10.1029/2019WR025380

Zhou, M., Xiong, L., Jiang, C., Chen, G., Liu, C., & Zha, X. (2024). River network-based index to clarify transmission of hydrological drought in reservoir-regulated basins. *Journal of Hydrology: Regional Studies*, *51*, 101604.

Zhu, Y., Zhou, Y., Xu, C. Y., & Chang, F. J. (2024). Optimising complementary operation of mega cascade reservoirs for boosting hydropower sustainability. *Sustainable Energy Technologies and Assessments*, *64*, 103719.

Zoccatelli, D., Wright, D. B., White, J. T., Fienen, M. N., & Yu, G. (2024). Precipitation uncertainty estimation and rainfall-runoff model calibration using iterative ensemble smoothers. *Advances in Water Resources*, 104658.